DRAFT SF 298

1. Report Date (dd-mm-yy)	2. Report Type	3. Dates covered (from... to)

4. Title & subtitle	5a. Contract or Grant #
Hydrogen Effects on Some Titanium Aluminides at Ambient Temperature Tri-Service Committee on Corrosion Proceedings	
	5b. Program Element #

6. Author(s)	5c. Project #
Mr. James A. Smith	5d. Task #
	5e. Work Unit #

7. Performing Organization Name & Address	8. Performing Organization Report #

9. Sponsoring/Monitoring Agency Name & Address	10. Monitor Acronym
Tri-Service Committee on Corrosion USAF WRIGHT-PATTERSON Air Force Base, Ohio 45433	11. Monitor Report #

12. Distribution/Availability Statement
Approved for Public Release
Distribution Unlimited

13. Supplementary Notes

14. Abstract

DTIC QUALITY INSPECTED 2

15. Subject Terms
Tri-Service Conference on Corrosion

Security Classification of			19. Limitation of Abstract	20. # of Pages	21. Responsible Person (Name and Telephone #)
16. Report	17. Abstract	18. This Page			

TRI-SERVICE
CONFERENCE
ON CORROSION

1994 TRI-SERVICE · DEPARTMENT OF DEFENSE · UNITED STATES OF AMERICA · CONFERENCE ON CORROSION

21-23 JUNE 1994

SHERATON PLAZA HOTEL
ORLANDO, FLORIDA

PROCEEDINGS

Hydrogen Effects on Some Titanium Aluminides at Ambient Temperature

Mr. James A. Smith
Naval Research Laboratory
Code 6314
Washington, DC 20375-5000

It is common to describe the corrosion damage of structural metals and alloys in terms of the eight basic types of metal/alloy corrosion: general corrosion, galvanic corrosion, crevice corrosion, pitting attack, erosion corrosion, selective leaching, intergranular corrosion, and environmental assisted fracture. The latter, environmental assisted fracture, may be further divided into subheadings of stress corrosion cracking, corrosion fatigue, and hydrogen embrittlement. Of particular interest is hydrogen embrittlement because of the serious problems and/or catastrophic failures that may result from the involvement of structural materials such as titanium and titanium alloys with hydrogen.

Previous investigators have shown that Ti-6Al-4V and indeed most conventional titanium alloys are susceptible to hydrogen embrittlement in hydrogen charging environments (22). Titanium aluminides, the materials studied in this report, are also believed to be subject to hydrogen embrittlement but preliminary studies show that the gamma based aluminides may be less prone to absorbing hydrogen at ambient and elevated temperatures than conventional Ti alloys (21). The major draw for use of these materials is the fact that they possess outstanding high-temperature strength, good creep behavior, and low density. Possession of these characteristics has warranted their consideration for a wide range of applications from automotive turbo charger motors, pistons, and valve material to advanced aerospace applications involving temperatures up to 1045^0C. Therefore, it is important to ascertain their hydrogen embrittlement behavior if hydrogen-related property damage is to be understood and, hopefully, controlled in these materials.

Experimental Overview

A. Materials

The material used in this study was produced by Martin Marietta Laboratory. The material was arc melted, cast in a chilled copper mold, forged, and annealed at approximately $1200^{o}C$. The TiB_2 particulate dispersion was introduced in situ using XD^{TM} processing (29). The chemical compositions of these cast materials are given in Table 1.

B.   Procedures

1.   Polarization Test
Polarization curves were measured at a sweep rate of 0.2 mV/s in deaerated 0.6N NaCl solutions, using a saturated calomel (SCE) reference electrode. The working electrode (~13 mm disc) was polished through 600 grit SiC paper, then cleaned and rinsed with distilled water, and finally degreased with acetone prior to use.

2.   Hydrogen Permeation Tests
Hydrogen permeation experiments were conducted on 1 mm thick discs using the electrochemical method. The experimental set-up, in Figure 1, shows an input chamber that contains the charging solution (0.6N NaCl) and a exit chamber that contains 0.2N NaOH. Both solutions were purged with high purity argon to remove dissolved oxygen. The permeation discs are surface ground on both sides thorough 600 grit paper and, subsequently, the exit surface is plated to provide several hundred angstroms of palladium. The purpose of the palladium plate is to provide a more uniform surface for the evolution of hydrogen and to provide the necessary surface conditions to ionize completely the hydrogen reaching the exit surface.

3.   CERT (constant extension rate testing)
All CERT (constant extension rate testing) studies were performed at room temperature using a Cortest constant extension testing machine at a strain rate of 1.45 x 10^{-6}/sec. Data acquisition and analyses were performed using a computer.

Results and Discussion

A.   Structure and Mechanical Properties:

Optical micrographs of cast Ti-48%Al with 5 Vol% and 10 Vol% TiB_2 are shown in Figs.2-3. The microstructures of these materials consists of a mixture of gamma (γ) grains and lamellar ($\gamma+\alpha_2$) grains. The TiB_2 particulate dispersion introduced in situ using XD^{TM} processing tends to grow in clusters and exhibits a blocky morphology .
For the investigated alloys, Ti-48%Al+5Vol%TiB_2 and Ti-48%Al+10 Vol% TiB_2, the mechanical properties of ultimate yield strength and % elongation together with the physical properties of diffusivity and permeation current density are listed in Table 2. The data show that the diffusivities of the two alloys are about the same, and that the alloy possessing the highest volume percentage of TiB_2 possesses the greater ultimate yield strength. It is further noted that the yield strengths for Ti-48%Al+5 Vol% TiB_2 and Ti-48%Al+10 Vol% TiB_2 decrease respectively, 16 and 20 % when cathodically polarized at -1400mV in 0.6N NaCl. Reductions in the % elongation resulting from hydrogen charging show even larger decreases approximately 43% for Ti-48%Al+5 Vol% TiB_2 and approximately 50%

for Ti-48%Al+10 Vol% TiB$_2$. These figures, however, are somewhat tentative because of the small values involved in the measurements.

B.   Polarization Study

Figure 4a. shows potentiodynamic polarization scans for the titanium aluminides reinforced with 5 Vol% TiB$_2$ and 10 Vol % of TiB$_2$. It is noted that an increase in the concentration of TiB$_2$ from 5 to 10 Vol% results in a significant diminution of the corrosion potential (Ecorr), shifting it approximately 685mV in the cathodic direction and creating an irregular passive region that extends from the active Ecorr value of alloy Ti-48%Al +10 Vol% TiB$_2$ to a value comparable to the more noble Ecorr value of Ti-48%Al+5 Vol% TiB$_2$. The Ti-48%Al+5 Vol% TiB$_2$ alloy does not possess a passive region but goes immediately into transpassive behavior under anodic polarization.

In Figure 4a., the broken lines represent cathodic reactions that are thermodynamically possible on titanium surfaces during cathodic polarization in near neutral 0.6N NaCl solutions . It is noted that the discontinuities viewed in the curve for the low TiB$_2$ material, alloy #82, correspond to the commencement of cathodic reactions as reported by Pourbaix (34). At , The discontinuity at approximately -700 mVcorresponds to the reaction $2H^+ + 2e^- \rightarrow H_2\uparrow$ and the discontinuity at approximately - 1300 mV, corresponds to the reaction $H_2O + e^- \rightarrow OH^- + 1/2\ H_2\uparrow$. Somewhat less distinct are the matchings of the cathodic reactions with discontinuities occurring in the cathodic polarization of alloy #83. It is suspected that increased chemical involvement of TiB$_2$ particulate at the higher TiB$_2$ particulate level causes the blurred matchings observed for this material.

In previous observations of cathodically charged titanium alloys in near neutral salt solutions it appeared that hydrogen was not readily absorbed by the titanium alloys even though the application of impressed current forced the potential well below the hydrogen evolution line (33). Hydrogen absorption, however, was found to occur naturally when the open circuit potential (Ecorr) of the metal or alloy resides in the region below the hydrogen evolution line as seen in Fig.4b. This condition is encountered at very high and very low pH values. For the high TiB$_2$ content material, alloy #83, the fact that the Ecorr value of -330 mV appears much closer to the $2H^+ + 2e^- \rightarrow H_2\uparrow$ evolution line than the Ecorr value of alloy #82 suggests that under cathodic charging there is a greater possibility of significant hydrogen uptake in this material than in the low TiB$_2$ content alloy #82.

In these TiB$_2$ containing Ti-48%Al alloys the effect of hydrogen appears to involve a complex interplay between the amount and accumulation of hydrogen at an interface and the size and distribution of the microstructural features. This effect is viewed as being composed of two factors:
1. Chemical
2. Microstructural.
The first factor is denoted by the decrease in E$_{corr}$ with increase in Vol% TiB$_2$ and the increase in cathodic Tafel slope with a decrease in Vol% TiB$_2$. Generally, the greater the magnitude of the cathodic Tafel slope the more difficult the reduction of

hydrogen. The second factor is denoted by the decrease in permeation current density (Table 2.) with increase in Vol% TiB_2. The latter observation suggests that hydrogen trapping may occur particularly in the alloy containing the higher TiB_2 content.

C.   Hydride Formation

Microhardness values across a Ti-48%Al+10 Vol%TiB_2 specimen after 720 hrs of H-permeation at -1400mv in 0.6N NaCl solutions showed significant increases at the specimen center (Fig.5). Xray diffraction analysis of this high hardness region indicated the presence of titanium hydride (Fig.6). Similar increases were not detected in the Ti-48%Al+5 Vol%TiB_2 alloy (Fig.7). This observation indicates that hydride formation is possible in this material and suggests that the presence and amount of hydride may depend on the concentration of TiB_2.

Hydride formation in Ti-48%Al+10 Vol%TiB_2 in 0.6N NaCl at -1400mV is noteworthy because these and similar alloys are being considered for such diverse applications as aerospace and automobile systems. The formation of TiH_x by cathodic polarization would limit their use as a structural materials. In view of the aforementioned observations, extreme care should be taken to guard against situations that subject these alloys to high cathodic currents for long periods of time.

The original purpose for the addition of TiB_2 to the TiAl base composition was to improve creep and "ductilize" the material. As the data show no significant benefits in ductility or fracture properties were obtained. The fracture mode remains transgranular cleavage for both the 5 and 10 Vol%TiB_2 material. Thus the addition of TiB_2 does not appear to preclude the occurrence of transgranular cleavage. The room temperature deformation behavior of the gamma titanium aluminides has been studied at this laboratory and others (25,35,36). These studies show that no well defined dislocation substructure is found in these materials, therefore, no persistent or recurrent slip band formation is expected. Thus, the classical model of crack initiation at recurrent/persistent slip bands and subsequent Stage I and Stage II crack growth does not hold true in these materials. It seems reasonable that microplastic deformation at stress levels close to the fracture stress and the absence of extensive activity of [011] and [101] easy-glide dislocations could easily lead to local stress concentrations. Such local stress concentrations could then initiate transgranular crack nucleation and propagation giving rise to the transgranular cleavage fracture seen in these materials. Additionally, in the case of the 10 Vol%TiB_2 material prolonged exposure to cathodic potentials could lead to the formation of hydrides which would further degrade material performance.

CONCLUSIONS

1.   Increasing the Vol% of TiB_2 from 5 to 10 % does not preclude the low temperature cleavage-like failure experienced by titanium aluminide alloy Ti-48%Al in air and aqueous salt solution.

2. Cathodic polarization in 0.6N NaCl solutions produces detectable amounts of titanium hydrides in alloy Ti-48%Al+10 Vol%TiB_2 after 720 hrs.

3. No hydrides are detected in the alloy containing 5 Vol% TiB_2.

4. Permeation data indicate low level hydrogen trapping in titanium aluminide alloy Ti-48%Al+10 Vol%TiB_2 after 720 hrs.

ACKNOWLEDGMENTS

REFERENCES

1. Hideki Hagi, Trans. of the Japan Institute of Metals, Vol. 27, No. 4, 233-240 (1986).
2. T. Tanabe, K. Sawada, and S. Imoto, Trans. of the Japan Institute of Metals, Vol. 27, No. 5, 321-327 (1986).
3. R. M. Latanision and M. Kurkela, Corrosion, Vol. 39, No. 5, 174-181 (1983).
4. Acta Metallurgica Sinica Series A, 4.
5. D. Warren, Material Performance, Vol. 26, No. 1, 38-45 (1987).
6. B. B. Pound, SRI International Final Report, #N00014-86-C-0233, (Nov 1990).
7. B. G. Pound, Corrosion, Vol. 45, 18-25 (1989).
8. R. B. Hutchings, A. Turnbull, and A. T. May, Scripta Metall. Mater., Vol. 25, 2657-2662 (1991).
9. N. Kishimoto, T. Tanabe, T. Suzuki, and H. Yoshida, Journal of Nuclear Materials, Vol. 127, 1-9 (1985).
10. Y. Y. Li and Z. S. Xing, Journal of Nuclear Materials, Vol. 169, 151-157 (1989).
11. R. Dus and M. Smialowski, Acta Metallurgica, Vol. 15, 1611-1616 (1967).
12. Morihiko Nakamura, Kenki Hashimoto, and Tokuzo Tsujimoto, Journal of Material Research, Vol. 8, No. 1, 68-77 (1993).
13. H. A. Lippsitt, "Titanium Alumindes An Overview," High Temperature Ordered Intermetallic Alloys, ed. C.C. Koch et al. (Boston, MA):Materials Research Society, 351-364 (1985).
14. S.M.L. Sastry, T.C. Peng and L.P. Beckeman, Metall. Trans. A, Vol. 15A, 1465-1474 (1984).
15. H.A. Lipsitt, Mat. Res. Soc. Symp. Proc., Vol. 39, Materials Research Society (1985).
16. C. Nishimura and C.T. Liu, Acta Metall Mater., Vol. 40, No.4, 723-731 (1992).

17. G.M. Camus, N.S. Stoloff, and D.J. Duquette, Acta Metall., Vol. 37, 1497 (1989).

18. C.T. Liu and M.T. Takayama, Scripta Metall. Mater., Vol. 24, 1583 (1990).

19. B.J. Berkowitz and C. Miller, Metall. Trans. 11A, 1877 (1980).

20. Jia Gao, Yan-Bin Wang, Wu-Yang Chu, and Chi-Mei Hsiao, Scripta Metall. Mater., Vol. 27, No. 9, 1219-1222 (1992).

21. C. T. Liu and Young-Won Kim, Scripta Metall. Mater., Vol. 27, No. 5, 599-603 (1992).

22. Y-W. Kim, Acta Metall. Mater., Vol. 40, 1121-1134, (1992)

23. W.Y. Chu and A.W. Thompson, Scripta Metall. Mater., Vol. 25, 641-644 (1991).

24. L.M. Pike and C.T. Liu, Scripta Metall. Mater., Vol. 27, 1313-1317 (1992).

25. Morihika Nakamura, Kennki Hashimoto, and Tokuzo Tsujimoto, submitted to J. Mater. Res., Vol. 8, 68-77, (1991).

26. E. Manor and D. Eliezer, Scripta Metall. Mater., Vol. 23, 1313-1318 (1989).

27. C.T. Liu, E.H. Lee, and C.G. Mckammey, Scripta Metall. Mater., Vol. 23 875, (1989).

28. C.T. Liu and W.C. Oliver, Scripta Metall. Mater., Vol. 25, 1933 (1991).

29. L. Christodoulou, P.A. Parrish, and C.R. Crowe, High Temperature/High Performance Composites, F.D. Lemkey, S.G. Fishman, A.G. Evans, and J.R. Strife,eds., MRS proc., MRS, Pittsburgh, PA, Vol. 120, pp. 29-34, (1988).

30. E. Smith and J.T. Barnby, Met. Sci. J., Vol. 1, 56,(1967).

31. H.A. Lipsitt, D. Shechtman, and R.E. Schafrik, Metall. Trans. A., Vol. 1A, 1369, (1980).

32. Fumio Hine, Masaki Yasuda, and Hitoshi Sato, Corrosion, Vol.33, No.5, 181-185, (1977).

33. R.E. Groover, J.A. Smith, and T.J. Lennox, Jr., Corrosion, Vol.28, No.3, pp.101-104, (1972).

34. M. Pourbaix, Corrosion, Vol.26, No.6, p267 (1969).

35. F. Appel, P. A. Beaven, and R. Wagner, Acta Metall. Mater., Vol. 41, No.6, 1721-1732 (1993).

36. C.R. Feng, D.J. Michel, and C.R. Crowe, Scripta Metall. Mater., Vol. 23 241-246, (1989).

TABLE 1.

Element (wt. %)

Alloy	Ti	Al	TiB_2 (Vol%)
#82	66	34	5
#83	66	34	10

TABLE 2.

Mat'l	Envir.	U.T Strength (MPa)	%El	Ecorr (mV)	Diffusivity (cm^2/sec)	H-Perm (nA/cm^2)	Fracture (Mode)
#82	Air	544.3	.14	-	-	-	clv
#82	-1400mV	457.2	.06	-	8.1×10^{-12}	39	clv
#82	0.6N NaCl	-	-	+355	-	-	clv
#83	Air	554.5	.12	-	-	-	clv
#83	-1400mV	443.6	.06	-	8.0×10^{-12}	35	clv
#83	0.6N NaCl	-	-	-330	-	-	clv

where:

#82 - Ti-48%Al+5 Vol% TiB_2
#83 - Ti-48%Al+10 Vol% TiB_2
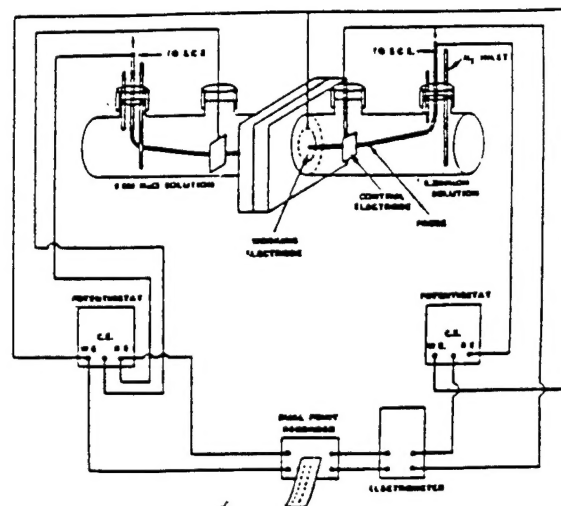
Fig. 1.   Experimental set-up for the permeation test.
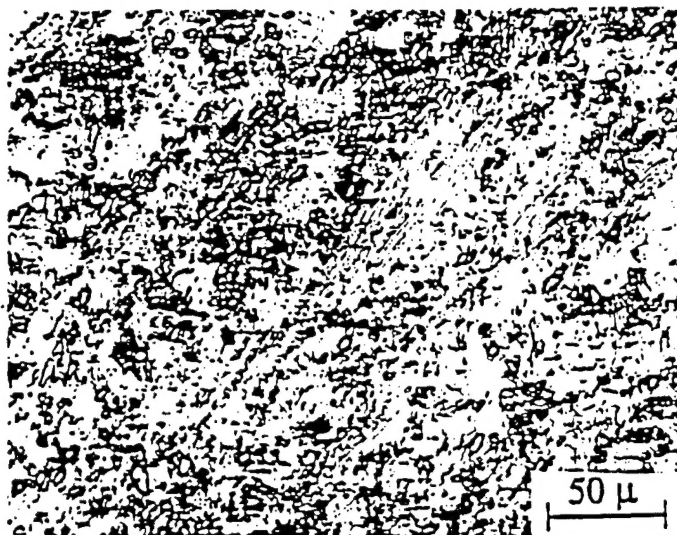
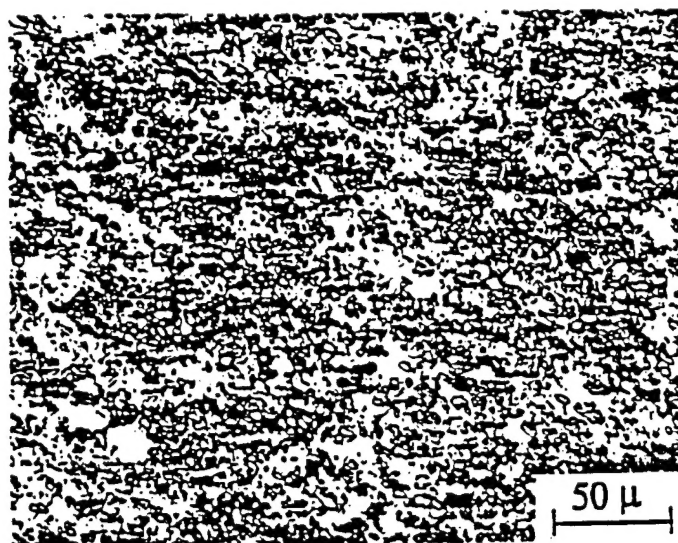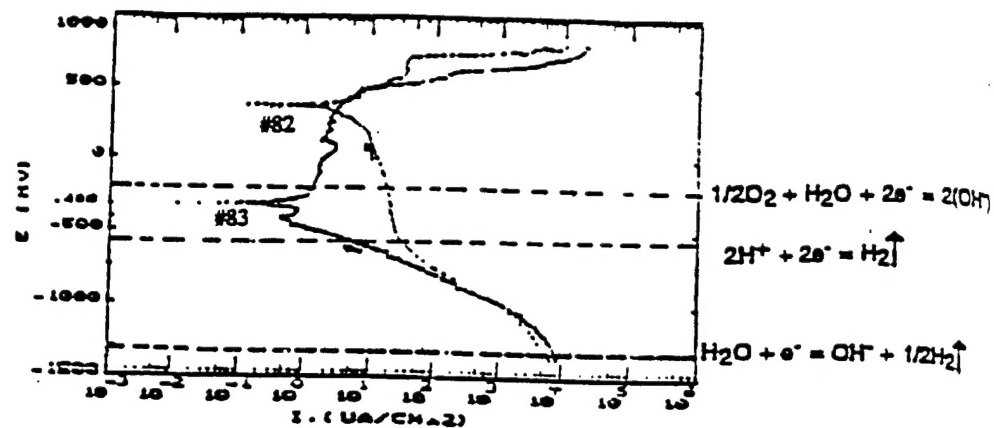Fig. 2. The microstructure of as-cast Ti-48%Al+5vol%TiB$_2$.

Fig. 3. The microstructure of as-cast Ti-48%Al+10vol%TiB$_2$.

9

Potentiodynamic polarization curves for Ti-48%Al alloys
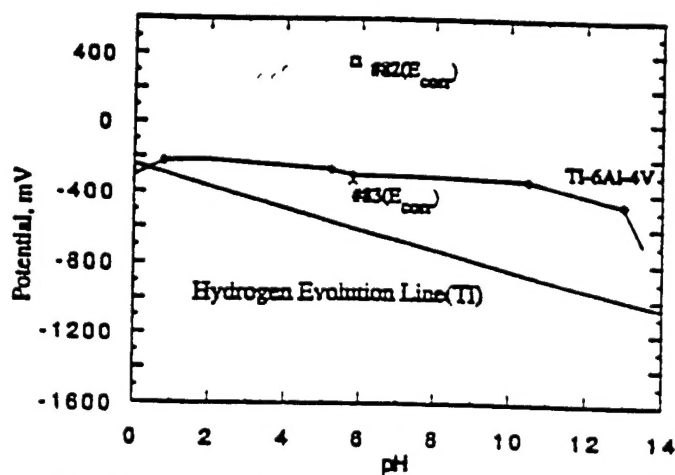Fig. 4a. with 5vol% and 10vol%TiB$_2$ in 0.6N NaCl at ambient temperature.

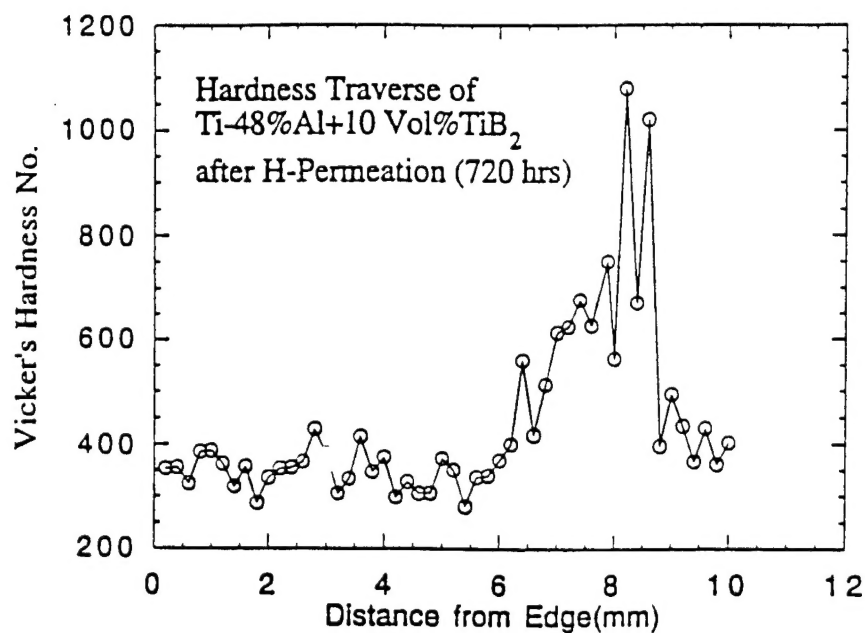Fig. 4b. Titanium aluminide potentials in 0.6N NaCl after 48 hrs.
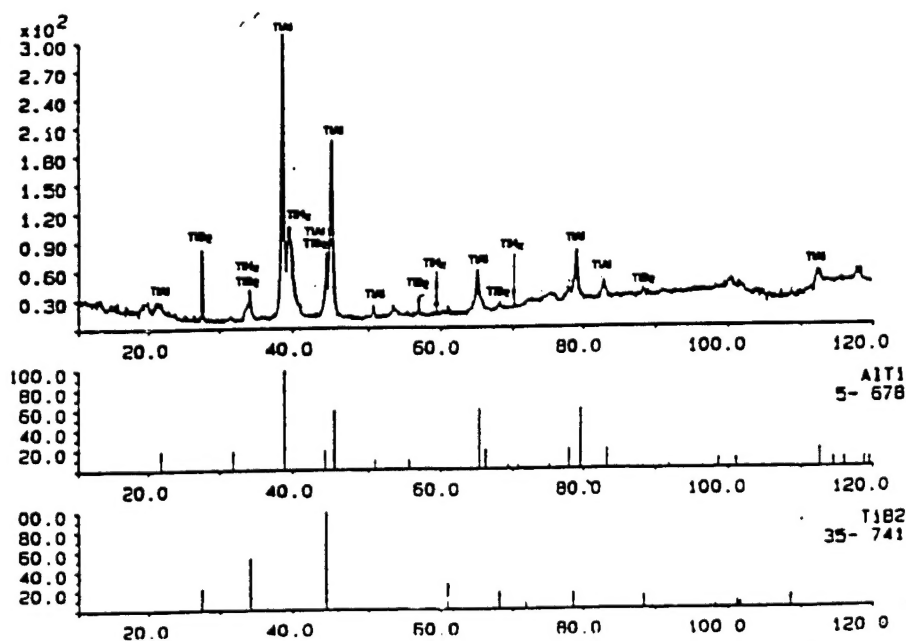
Fig. 5. Hardness traverse for Ti-48%Al+10 Vol%TiB$_2$

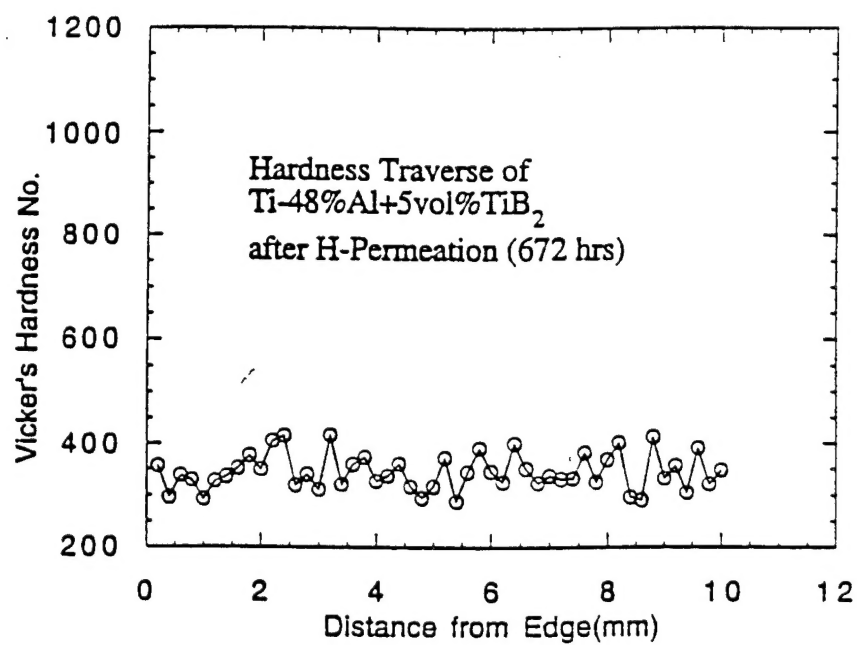Fig. 6. X-ray diffraction pattern of Ti-48%Al+10 Vol% TiB$_2$
after H-permeation in 0.6N NaCl for 720 hrs.

Fig. 7.   Hardness traverse for Ti-48%Al+5 Vol% TiB$_2$

12